Comparison between Different DPC Methods Applied to DFIG Wind Turbines

Seyed Mohammad Tavakoli*‡, Mohammad Ali Pourmina*, Mohammad Reza Zolghadri**

* Department of Electrical Engineering, Science and Research Branch, Islamic Azad University, Tehran, Iran

** Department of Electrical Engineering, Sharif University of Technology, Tehran, Iran

mota4099@yahoo.com, pourmina@srbiau.ac.ir, zolghadr@sharif.edu

‡ Corresponding Author; Seyed Mohammad Tavakoli, Department of Electrical Engineering, Science and Research Branch, Islamic Azad University, Tehran, Iran, +989198005862, mota4099@yahoo.com

Received: 23.04.2013 Accepted: 25.05.2013

Abstract- In this paper the direct power control methods of doubly fed induction generator in wind turbine applications are studied. In the methods under study, the proper voltage space vector of the rotor side converter is selected using a switching table which is derived from flux position and the difference between the measured and reference stator active and reactive powers. Various simulations are performed in Matlab/Simulink software on a DFIG system in order to investigate the dynamic performance and robustness of the proposed control methods against machine internal parameters variations.

Keywords- Direct Power Control (DPC), Doubly Fed Induction Generator (DFIG), Rotor Side Converter (RSC), Space Vector, Wind Turbine.

1. Introduction

In recent years there has been a growing research on application of variable speed systems in wind turbine applications due to their higher efficiency compared to fixed speed systems and the possibility of capturing maximum power from the wind. Among various common variable speed wind turbine schemes the Doubly Fed Induction Generator (DFIG) is of great importance. As shown in Fig. 1, the stator is connected directly to the grid while the rotor is connected via a power electronics converter. This structure results in a lower rating of the converter, about 20-30% of the nominal power of the generator, which reduces the cost and size of the converter in turn.

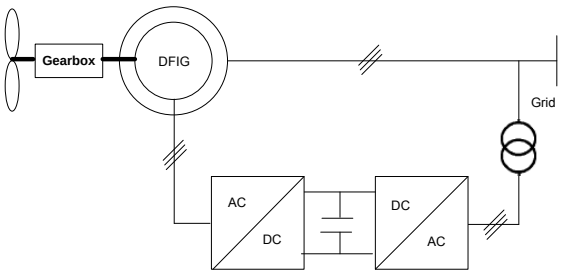

Fig. 1. Structure of a DFIG connected to the grid.

Several control methods have recently been proposed for DFIG, the control variables being stator active and reactive powers. In some researches torque [1-2] or speed [3] have been controlled instead of active power. Taking into account that the active power is related to the torque and the speed, the different control methods share the same objective.

The traditional control method of DFIG is the field oriented control (FOC) or flux vector control, where the stator active and reactive powers of DFIG are controlled using current controller blocks [4-5]. Although the flux vector control has several advantages to scalar control methods it has some demerits. The control system is complex and its implementation is difficult due to need of reference frame transformation and flux orientation. Moreover, exact values of internal parameters of the machine including inductances and resistances is required. The performance of the control system can therefore be affected with the change of internal parameters of the machine from their nominal values.

With the advent of the Direct Torque Control (DTC) method for induction motors in 1986, this method has been applied to control of DFIG [6-7]. The DTC method has some important advantages to the FOC method such as simpler control structure, faster dynamic response and low

dependence on machine internal parameters. The torque and flux are controlled directly without current control blocks.

The Direct Power Control (DPC) method has recently been proposed for control of DFIG based on a similar idea as the DTC method [8-9]. In this approach the active and reactive powers of stator are controlled directly which leads to a very fast dynamic response. A DPC method of DFIG has been proposed in [8] which does not need reference frame transformation and flux orientation making its implementation easier than the FOC method. This method needs rotor flux estimation. As the DFIG operates with a low rotor slip, rotor flux estimation is difficult making the precision of the control system dependant on internal parameters of the machine. Several years later, another DPC method of DFIG was proposed in [9] which does not need rotor flux estimation solving the problem in low slip speeds. This second method is based on stator flux estimation in the rotor reference frame.

In this paper a comparison is made between DPC methods of DFIG in terms of dynamic performance and robustness to variation of internal machine parameters when the rotor speed and reference values of stator active and reactive powers change. This study can be used to compare different control methods in terms of dynamic performance and robustness.

2. Dynamic model of DFIG in the rotor reference frame

The stator and rotor voltage space vector equations are expressed in the rotor reference frame rotating with speed ω_r as follows:

$$V_s^r = R_s I_s^r + \frac{d\psi_s^r}{dt} + j\omega_r \psi_s^r$$
$$V_r^r = R_r I_r^r + \frac{d\psi_r^r}{dt} \quad (1)$$

The stator and rotor flux space vectors are:

$$\psi_s^r = L_s I_s^r + L_m I_r^r$$
$$\psi_r^r = L_r I_r^r + L_m I_s^r \quad (2)$$

In Eq. (1) and Eq. (2) $V, I, \psi, \omega_r, R, L$ are the voltage, current, flux, angular speed, resistance and inductance, respectively. s and r stand for the stator and rotor reference frames. The space vectors of stator and rotor flux in stationary stator and rotating rotor reference frames are shown in Fig. 2.

The stator current can be expressed as following using stator and rotor flux equations [9]:

$$I_s^r = \frac{L_r \psi_s^r - L_m \psi_r^r}{L_s L_r - L_m^2} = \frac{\psi_s^r}{\sigma L_s} - \frac{L_m \psi_r^r}{\sigma L_s L_r}$$
$$\sigma = \frac{L_s L_r - L_m^2}{L_s L_r} \quad (3)$$

where σ is the leakage factor.

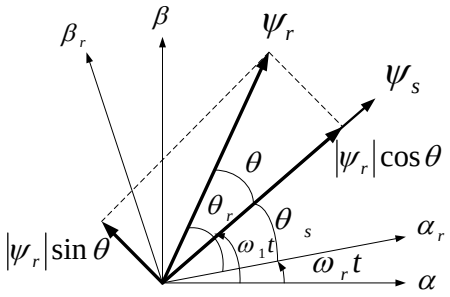

Fig. 2. The space vectors of stator and rotor flux different reference frames [9].

The input active power to the machine and output reactive power to the grid can be calculated directly using stator voltage and current space vectors as follows:

$$P_s = \frac{3}{2} V_s^r \cdot I_s^r \quad (4)$$

$$Q_s = -\frac{3}{2} V_s^r \times I_s^r \quad (5)$$

Where (.) and (×) represent dot product and vector product, respectively.

Inserting Eq. (1) and Eq. (3) in Eq. (4) and Eq. (5), stator active and reactive powers are obtained as follows [9]:

$$P_s = -\frac{3}{2} \frac{L_m}{\sigma L_s L_r} \omega_1 |\psi_s^r| |\psi_r^r| \sin\theta \quad (6)$$

$$Q_s = \frac{3}{2} \frac{\omega_1}{\sigma L_s} |\psi_s^r| \left(\frac{L_m}{L_r} |\psi_r^r| \cos\theta - |\psi_s^r| \right) \quad (7)$$

Where θ is the angle between stator and rotor flux space vectors as shown in Fig. 2.

3. Direct Power Control Methods of DFIG

The stator active and reactive powers are directly controlled in the DPC method. It can be concluded from Eq. (6) and Eq. (7) that stator active and reactive powers can be varied by changing the amplitudes of stator and rotor flux space vectors and the angle between them. Assuming the stator voltage is maintained constant by the grid and the rotor speed does not change during the sampling interval, differentiation of Eq. (6) and Eq. (7) with respect to time leads to:

$$\frac{dP_s}{dt} = -\frac{3}{2} \frac{L_m}{\sigma L_s L_r} \omega_1 |\psi_s^r| \frac{d\left(|\psi_r^r| \sin\theta\right)}{dt} \quad (8)$$

$$\frac{dQ_s}{dt} = \frac{3}{2} \frac{\omega_1}{\sigma L_s} |\psi_s^r| \frac{d\left(|\psi_r^r| \cos\theta\right)}{dt} \quad (9)$$

The stator active and reactive powers can then be varied by changing the components of rotor flux space vector

perpendicular and in the same direction of stator flux space vector, being $\left|\psi_r^r\right|\sin\theta$ and $\left|\psi_r^r\right|\cos\theta$, respectively, which are depicted in Fig. 2.

Neglecting the resistive drop on the rotor resistance yields:

$$\frac{d\left|\psi_r^r\right|}{dt} = V_r^r - R_r I_r^r \approx V_r^r \tag{10}$$

This shows that the rotor flux space vector can be manipulated by varying the rotor voltage space vector. The stator and rotor fluxes are calculated in each sampling interval using the following equations:

$$\psi_s^s = \int (V_s^s - R_s I_s^s)dt \tag{11}$$

$$\psi_r^r = \int (V_r^r - R_r I_r^r)dt \tag{12}$$

Assuming a two-level Voltage Source Converter (VSC) is feeding the rotor of DFIG, rotor voltage space vectors divide the space to 6 regions as shown in Fig. 3. These vectors are categorized to nonzero (V1-V6) and zero (V0 and V7) groups.

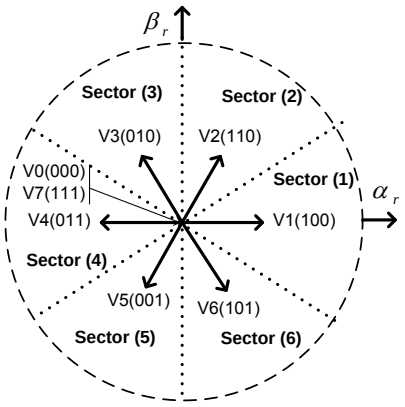

Fig. 3. Rotor voltage space vectors.

The effect of each rotor voltage space vector on rotor flux and thus Ps and Qs can then be determined in all the six regions by determining the position of flux space vector in the rotor reference frame. In each region, four out of the total six nonzero rotor voltage space vectors either increase or decrease the stator active and reactive powers, while the remaining two vectors increase the active power in half of the plane and decrease it in the other half and either increase or decrease the reactive power (or vice versa).

The DPC control methods can be divided to two groups whether the rotor or stator flux is estimated.

3.1. Rotor Flux Estimation Based DPC Method

In the rotor flux estimation based DPC method the proper rotor voltage space vector is selected using a switching table based on the rotor flux position in the rotor reference frame and the difference between measured and reference stator active and reactive powers. The structure of the rotor flux estimation based DPC method is presented in Fig. 4. Two 2-level hysteresis comparators are used as in Fig. 5 to compare the measured values of stator active and reactive powers with their reference values.

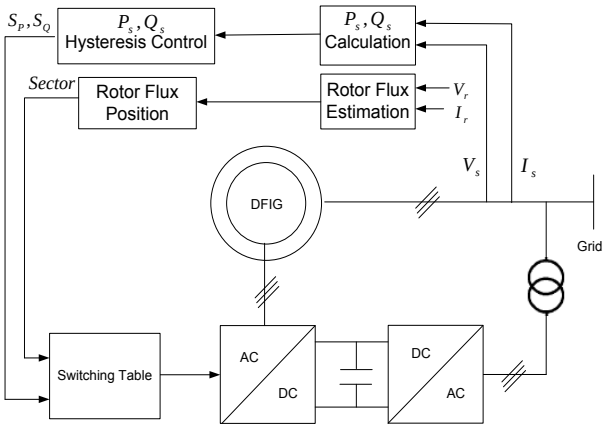

Fig. 4. The structure of the rotor flux estimation based DPC method.

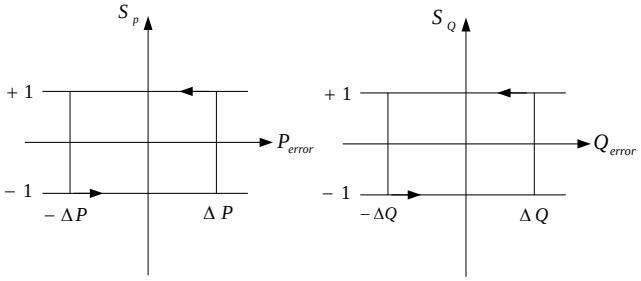

Fig. 5. Switching pattern of the two 2-level active-reactive power hysteresis comparators.

The increasing or decreasing effect of four of the rotor voltage space vectors on Ps and Qs for different positions of rotor flux space vector is shown in Table 1. Symbol K refers to the region where the rotor flux space vector is located.

Table 1. Increasing or Decreasing Effect of the Four Nonzero Rotor Voltage Space Vectors on Stator Active and Reactive Powers

Q_S \ P_S	↑	↓
↑	V_{K-1}	V_{K+1}
↓	V_{K-2}	V_{K+2}

The switching table for rotor flux estimation based DPC method can be extracted as in Table 2 using the rotor flux position in the rotor reference frame and output signals of the hysteresis comparators together with Table 1. After selection of the proper rotor voltage space vector using the switching table, the associated command pulses with the selected vector are sent to switch the RSC.

Table 2. Switching Table for Rotor Flux Estimation Based DPC

Sector		1	2	3	4	5	6
S_P=1	S_Q=1	V_6	V_1	V_2	V_3	V_4	V_5
	S_Q=-1	V_5	V_6	V_1	V_2	V_3	V_4
S_P=-1	S_Q=1	V_2	V_3	V_4	V_5	V_6	V_1
	S_Q=-1	V_3	V_4	V_5	V_6	V_1	V_2

3.2. Stator Flux Estimation Based DPC Method

In the stator flux estimation based DPC method, the proper rotor voltage space vector is selected based on the optimal switching table extracted from stator flux position in the rotor reference frame and the difference between measured and reference stator active and reactive powers. The structure of the control system is shown in Fig. 6. Two 3-level hysteresis comparators as in Fig. 7 are incorporated in order to compare the measured stator active and reactive powers with their respective reference values.

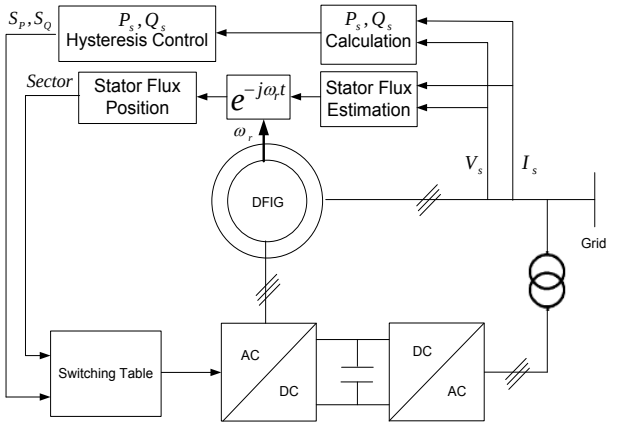

Fig. 6. The structure of the stator flux estimation based DPC method.

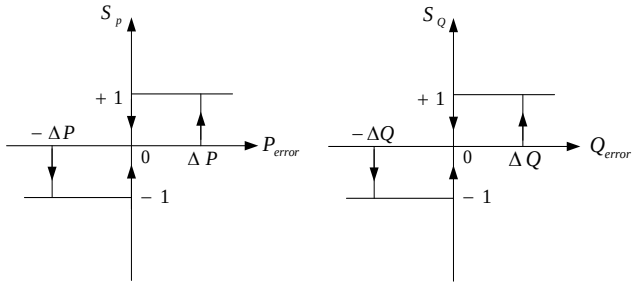

Fig. 7. Switching pattern of the two 3-level active-reactive power hysteresis comparators [9].

The effect of all six nonzero rotor voltage space vectors on stator active and reactive powers based on the position of stator flux space vector is presented in Table 3 for all the six sectors.

Table 3. Increasing or Decreasing Effect of All the Six Rotor Voltage Space Vectors on Stator Active and Reactive Powers

Sector		1	2	3	4	5	6
V_1	P_S	↑↓	↑	↑	↓↑	↓	↓
	Q_S	↑	↑	↓	↓	↓	↑
V_2	P_S	↓	↑↓	↑	↑	↓↑	↓
	Q_S	↑	↑	↑	↓	↓	↓
V_3	P_S	↓	↓	↑↓	↑	↑	↓↑
	Q_S	↓	↑	↓	↑	↓	↓
V_4	P_S	↓↑	↓	↑	↑↓	↑	↑
	Q_S	↓	↓	↑	↑	↑	↓
V_5	P_S	↑	↓↑	↓	↓	↑↓	↑
	Q_S	↓	↓	↓	↑	↑	↑
V_6	P_S	↑	↑	↓↑	↓	↓	↑↓
	Q_S	↑	↓	↓	↓	↑	↑

Taking into account the fact that the zero rotor voltage space vectors (V0 and V7) have no effect on the rotor flux, Eq. (8) and Eq. (9) can be rewritten as follows [9]:

$$\frac{dP_S}{dt} = \frac{3}{2}\frac{L_m}{\sigma L_s L_r}\omega_1 \left|\psi_s^r\right|\left|\psi_r^r\right|\cos\theta(\omega_1 - \omega_r) \tag{13}$$

$$\frac{dQ_S}{dt} = \frac{3}{2}\frac{\omega_1}{\sigma L_s}\left|\psi_s^r\right|\left|\psi_r^r\right|\sin\theta(\omega_1 - \omega_r) \tag{14}$$

The angle between stator and rotor flux space vectors (θ) is positive in the generating mode. Therefore, application of zero rotor voltage space vectors in all the six sectors increases stator active and reactive powers in sub-synchronous speeds and reduces stator active and reactive powers in super-synchronous speeds.

Knowing the position of stator flux in the rotor reference frame and the outputs of hysteresis comparators together with Table 3 and taking into account the effect of zero rotor voltage space vectors on Ps and Qs, the optimal switching table for stator flux estimation based DPC method is extracted as in Table 4. Similar to the previous DPC method the associated command pulses with the selected vector are sent to switch the RSC.

Table 4. Optimal Switching Table for Stator Flux Based DPC Method

Sector		1	2	3	4	5	6
S_P=1	S_Q=1	V_6	V_1	V_2	V_3	V_4	V_5
	S_Q=0	V_5	V_6	V_1	V_2	V_3	V_4
	S_Q=-1	V_5	V_6	V_1	V_2	V_3	V_4
S_P=0	S_Q=1	V_1	V_2	V_3	V_4	V_5	V_6
	S_Q=0	V_0	V_7	V_0	V_7	V_0	V_7
	S_Q=-1	V_4	V_5	V_6	V_1	V_2	V_3
S_P=-1	S_Q=1	V_2	V_3	V_4	V_5	V_6	V_1
	S_Q=0	V_3	V_4	V_5	V_6	V_1	V_2
	S_Q=-1	V_3	V_4	V_5	V_6	V_1	V_2

4. Simulation Results

Various simulations have been performed using Matlab/Simulink software in order to study and compare the aforementioned DPC methods. The parameters of the simulated DFIG are presented in Table 5. The grid frequency is 50 HZ while the sampling frequency is 20 KHZ. The DC link voltage is set at 250 V while the rated stator voltage is 380 V. The RSC is not connected to the rotor in the first 0.2 seconds in order that the DC link voltage builds up to the desired value.

The rotor speed varies linearly in the interval 0.6 to 0.8 seconds from -20% of synchronous speed (126 rad/sec) to 20% of synchronous speed (188 rad/sec). The reference active power is changed as a step function at t=0.4 sec from -70 W to the nominal power being -270 W and then at t=1 sec from -270 W to -70 W. The reference value of reactive power has been kept constant at zero.

Table 5. Parameters of the Simulated DFIG

Parameter	R_s	L_s	R_r	L_r	L_m	pp	P_n
Value	8.55 Ω	0.684 H	0.67 Ω	0.0536 H	0.148 H	2	270 W

The study firstly investigates the dynamic performance of the control methods and then their robustness against internal machine parameters.

4.1. Dynamic performance

The control system performances during rotor speed and reference stator active and reactive power variations have been demonstrated in Fig. 8. It is visible from the simulation results that the stator active and reactive powers have tracked their reference values after a step change in the references well in a few milliseconds in both the DPC methods. Changes in the rotor speed don't affect the control system performance in either of the two methods. It can therefore be concluded that the dynamic performance of both of the DPC methods is proper and fast enough. It can also be observed from comparison of the waveforms of the two methods that stator active and reactive power ripples have been greatly reduced by application of stator flux estimation based DPC in comparison with rotor flux estimation based DPC. This decrease in ripple is due to the increase in the number of nonzero rotor voltage space vectors in the switching table of stator flux estimation based DPC.

Harmonic spectrum of the stator current for the two DPC methods has been shown in Fig. 9. It is visible that the harmonic content of stator current has decreased greatly in the stator flux estimation based DPC in comparison with rotor flux estimation based DPC. Quantitative results of the simulations have been presented in Table 6 in order to have a better comparison of DPC methods.

Table 6. Quantitative Performance Comparison

method / feauture	rotor flux estimation based DPC	stator flux estimation based DPC
Transitory Response (negative and positive references step: P_S)	5 ms	5 ms
active power ripple	± 10 W	± 5 W
reactive power ripple	± 30 Var	± 5 Var
stator current Total Harmonic Distortion (THD)	2.56 %	0.79 %

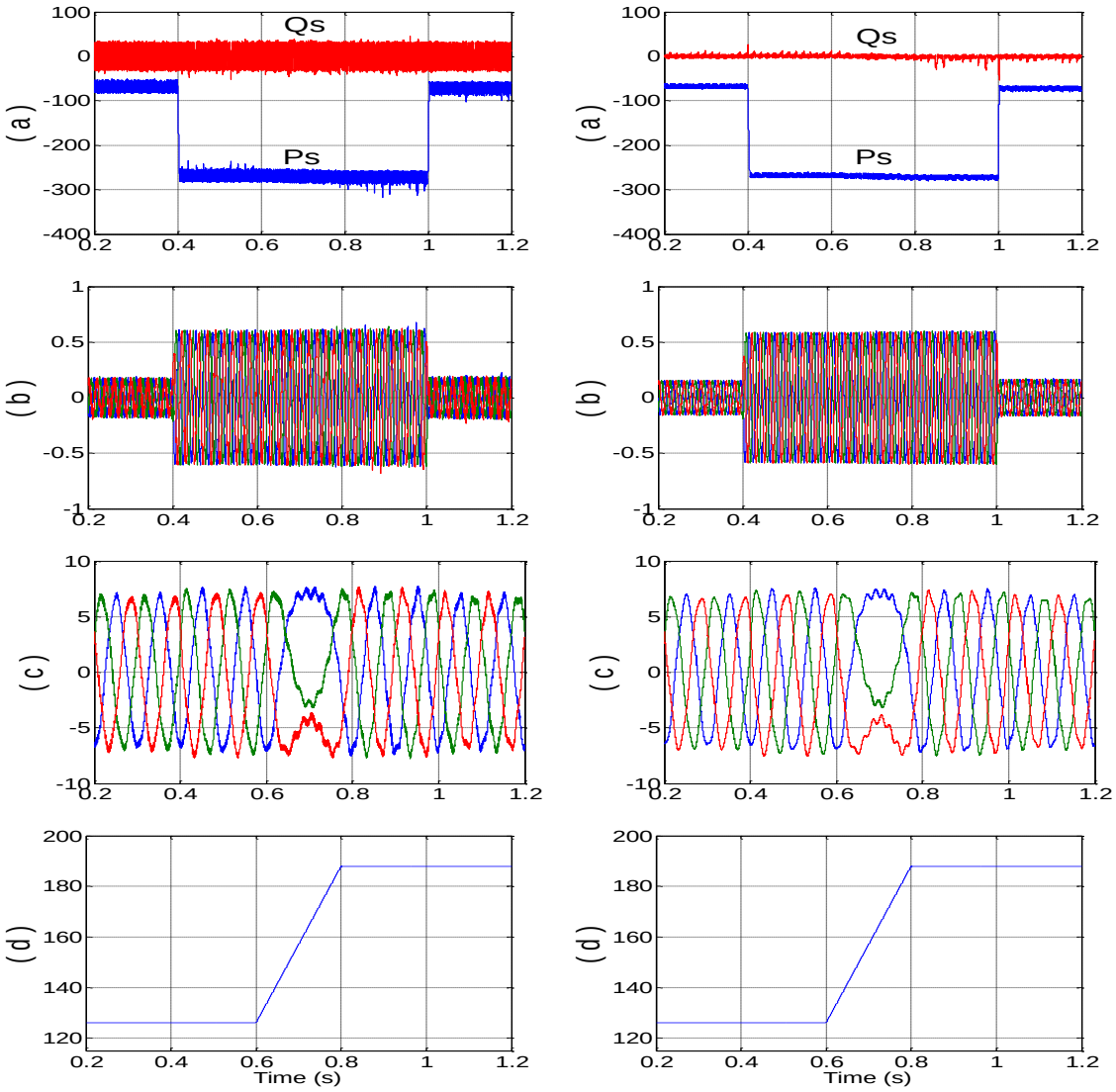

Fig. 8. Simulated results under various rotor speed and reference stator active and reactive powers (A) rotor flux estimation based DPC (B) stator flux estimation based DPC: (a) stator active power (W) and reactive power (Var), (b) stator current (A), (c) rotor current (A) and (d) rotor speed (rad/sec).

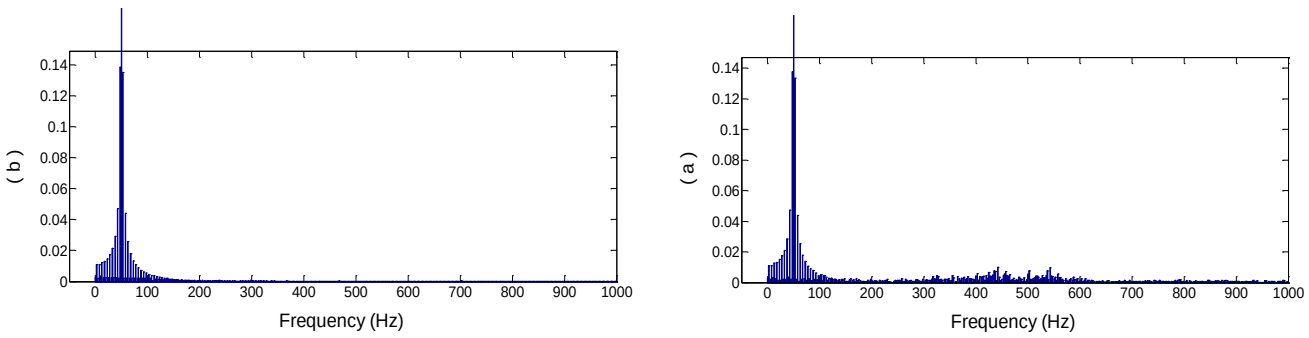

Fig. 9. stator current harmonic spectrum: (a) rotor flux estimation based DPC and (b) stator flux estimation based DPC.

4.2. Robustness against internal machine parameters

The only internal machine parameter value needed in rotor flux estimation and stator flux estimation based DPC is rotor and stator resistance respectively. In order to investigate the robustness of the two methods, the values of the corresponding resistances have been changed by 20% above their nominal values. Variation of the other machine parameters doesn't affect the control system performance and their values are not needed.

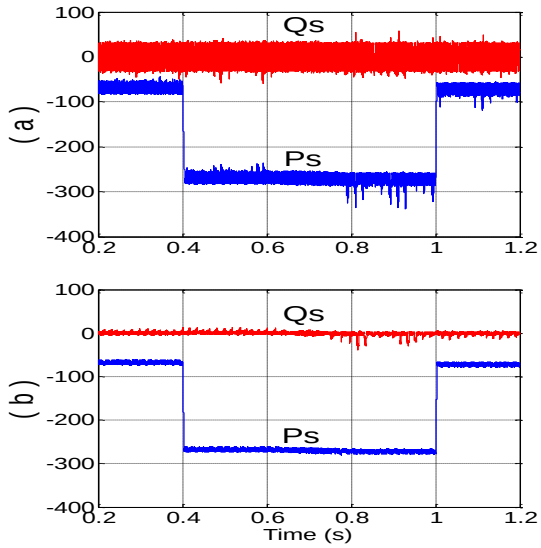

Fig. 10. Simulated results under various rotor speed and reference stator active and reactive powers and with internal machine parameters variation (a) rotor flux estimation based DPC (b) stator flux estimation based DPC.

Control system response to the change of internal machine parameters during rotor speed and reference stator active and reactive powers variation for the two DPC methods is presented in Fig. 10. It is observed from Fig. 10a that stator active and reactive powers mostly keep well in their hysteresis band in the rotor flux estimation based DPC method instead of the great change of rotor resistance from its nominal value; however, the active power has largely gone out of the hysteresis band in some instants. As is shown in Fig. 10b the stator active and reactive powers are always well inside the hysteresis band instead of the change in stator resistance from its nominal value. It can thus be concluded that the stator flux estimation based DPC is more robust against internal machine parameters in comparison with rotor flux estimation based DPC.

5. Conclusion

In this paper the DPC methods of DFIG in wind turbine applications were theoretically studied and simulated. It can be concluded from simulation results that the dynamic performance of the DPC methods is precise and very fast. Of course, stator active and reactive power ripples and harmonic content of stator current are highly lower in stator flux estimation based DPC in comparison with rotor flux estimation based DPC. Moreover, the stator flux estimation based DPC is more robust against internal machine parameters variations than the rotor flux estimation based DPC for low slip speeds. It is also observed in all the simulations that the control system always keeps stable during rotor speed and reference stator active and reactive power variations.

References

[1] L. Xu and W. Cheng, "Torque and reactive power control of a doubly fed induction machine by position sensorless scheme", IEEE Trans. on industry applications, Vol. 31, No. 3, pp. 636-642, May/June 1995

[2] N. P. Quang, A. Dittrich and A. Thieme, "Doubly fed induction machine as generator: Control algorithms with decoupling of torque and power factor", Electrical Engineering 80 (1997), Springer- verlag 197, Vol. 80, No. 5, pp. 325-335, 1997

[3] S. Peresada, A. Tilli and A.Tonielli, "Robust output feedback control of a doublyfed induction machine", IEEE 25th annual conference on industrial electronics, Vol. 3, No. 1, pp. 1348-1354, November 1999

[4] S. Muller, M. Deicke and R. W. De Doncker, "Doubly fed induction generator systems for wind turbines", IEEE Industry Applications, vol. 17, No. 1, pp. 26-33, May/Jun 2002

[5] Chia Chi Chu, Chia Chun Hung, Yuan Zheng Lin and ZenJey Guey, "Universal field oriented rotor side controllers for doubly fed induction generators", International Conference on Power Electronics and Drive Systems, pp. 342-347, 2009

[6] K. Gierlotka and M. Jelen, "Control of double-fed induction machine using DTC method", in Proc. EDPE'03, pp476-481, September 2003, Slovakia

[7] U. Baader, M. Depenbrock and G. Gierse, "Direct self control (DSC) of inverter-fed induction machine: A basis for speed control without speed measurement", IEEE Trans. Industry Applications, Vol. 28, pp. 581-588, May/June 1992

[8] Rajib Datta and V. T. Ranganathan, "Direct power control of grid connected wound rotor induction machine without rotor position Sensors", IEEE Trans. Power Electronics, Vol. 16, No. 3, May 2001

[9] Lie Xu and Phillip Cartwright, "Direct active and reactive power control of DFIG for wind energy generation", IEEE Trans. Energy Conversion, Vol. 21, No. 3, Sep 2006